*Supporting Information*

# Generalised predictability in the synthesis of biocarbons as clean energy materials: Targeted high performance CO₂ and CH₄ storage

Ibtisam Alali, and Robert Mokaya*

School of Chemistry, University of Nottingham, University Park, Nottingham NG7 2RD, U. K.

*E-mail: r.mokaya@nottingham.ac.uk (R. Mokaya)*

Table S1. $CO_2$ uptake of various porous carbons at 25 °C and 0.15 bar or 1 bar (Table adapted from reference 34 in main manuscript).

| | CO$_2$ uptake (mmol/g) | | Reference |
| --- | --- | --- | --- |
| | 1 bar | 0.15 bar | |
| Sawdust-derived activated carbon | 4.8 | 1.2 | 1 |
| KOH-activated templated carbons | 3.4 | ~1.0 | 2 |
| Petroleum pitch-derived activated carbon | 4.55 | ~1.0 | 3 |
| Activated carbon spheres | 4.55 | ~1.1 | 4 |
| Phenolic resin activated carbon spheres | 4.5 | ~1.2 | 5 |
| Poly(benzoxazine-co-resol)-derived carbon | 3.3 | 1.0 | 6 |
| Fungi-derived activated carbon | 3.5 | ~1.0 | 7 |
| Chitosan-derived activated carbon | 3.86 | ~1.1 | 8 |
| Polypyrrole derived activated carbon | 3.9 | ~1.0 | 9 |
| Soya bean derived N-doped activated carbon | 4.24 | 1.2 | 10 |
| N-doped ZTCs | 4.4 | ~1.0 | 11 |
| Activated templated N-doped carbon | 4.5 | 1.4 | 12 |
| Polyaniline derived activated carbon | 4.3 | 1.38 | 13 |
| N-doped activated carbon monoliths | 5.14 | 1.25 | 14 |
| Activated N-doped carbon | 3.2 | 1.5 | 15 |
| Activated hierarchical N-doped carbon | 4.8 | 1.4 | 16 |
| Activated N-doped carbon from algae | 4.5 | ~1.1 | 17 |
| Compactivated carbons from sawdust | 5.8 | 2.0 | 18 |
| Fern-derived activated carbon | 5.67 | ~1.7 | 19 |
| Compactivated carbons from polypyrrole | 5.5 | 2.1 | 20 |

**References**
1. M. Sevilla and A. B. Fuertes, *Energy Environ. Sci.*, 2011, **4**, 1765.
2. M. Sevilla and A. B. Fuertes, *J. Colloid Interface Sci.*, 2012, **366**, 147.
3. J. Silvestre-Albero, A. Wahby, A. Sepulveda-Escribano, M. Martinez-Escandell, K. Kaneko and F. Rodriguez-Reinoso, *Chem. Commun.*, 2011, **47**, 6840.
4. N. P. Wickramaratne and M. Jaroniec, *ACS Appl. Mater. Interfaces*, 2013, **5**, 1849.
5. N. P. Wickramaratne and M. Jaroniec, *J. Mater. Chem. A*, 2013, **1**,112.
6. G. P. Hao, W. C. Li, D. Qian, G. H. Wang, W. P. Zhang, T. Zhang, A. Q. Wang, F. Schuth, H. J. Bongard and A. H. Lu, *J. Am. Chem. Soc.*, 2011, **133**, 11378.
7. J. Wang, et al, *J. Mater. Chem.*, 2012, **22**, 13911.
8. X. Fan, L. Zhang, G. Zhang, Z. Shu, J. Shi, *Carbon*, 2013, **61**, 423.
9. M. Sevilla, P. Valle-Vigon and A. B. Fuertes, *Adv. Funct. Mater.*, 2011, **21**, 2781.
10. W. Xing, et al, *Energy Environ. Sci.*, 2012, **5**, 7323.
11. Y. D. Xia, R. Mokaya, G. S. Walker and Y. Q. Zhu, *Adv. Energy Mater.*, 2011, **1**, 678.
12. Y. Zhao, L. Zhao, K. X. Yao, Y. Yang, Q. Zhang and Y. Han, *J. Mater. Chem.*, 2012, **22**, 19726.
13. Z. Zhang, et al, *Phys.Chem. Chem. Phys.,* 2013, **15**, 2523
14. M. Nandi, et al, *Chem. Commun.,* 2012, **48**, 10283.
15. M. Saleh, J. N. Tiwari, K. C. Kemp, M. Yousuf and K. S. Kim, *Environ. Sci. Technol.*, 2013, **47**, 5467.
16. D. Lee, C. Zhang, C. Wei, B. L. Ashfeld and H. Gao, *J. Mater. Chem. A*, 2013, **1**, 14862.
17. M. Sevilla, C. Falco, M. M. Titirici and A. B. Fuertes, *RSC Advances*, 2012, **2**, 12792.
18. N. Balahmar, A. C. Mitchell, and R. Mokaya, *Adv. Energy Mater.*, 2015, **5**, 1500867.
19. J. Serafin, K. Kiełbasa and, B. Michalkiewicz, *Chem. Eng. J.*, 2022, **429**, 131751.
20. B. Adeniran and R. Mokaya, *Nano Energy*, 2015, **16**, 173.

Table S2. Packing (or tapping) density and low-pressure volumetric $CO_2$ uptake, expressed as g l$^{-1}$ (or cm$^3$ (STP) cm$^{-3}$), for clove-derived activated carbons compared to benchmark carbons and metal organic frameworks (MOFs). The values in parenthesis are volumetric uptake expressed as cm$^3$ (STP) cm$^{-3}$.

| Sample | Density[a] (g cm$^{-3}$) | Volumetric $CO_2$ uptake (g l$^{-1}$) or (cm$^3$ STP cm$^{-3}$) | | | | Reference |
|---|---|---|---|---|---|---|
| | | 0.15 bar | 1 bar | 5 bar | 9 bar | |
| ACC2600 | 0.92 | 45 (23) | 182 (93) | 390 (199) | 463 (236) | This work |
| ACC2700 | 0.79 | 38 (19) | 170 (87) | 400 (204) | 482 (245) | This work |
| ACC2800 | 0.72 | 29 (15) | 133 (68) | 349 (178) | 450 (229) | This work |
| HCC2600 | 0.98 | 56 (29) | 185 (94) | 353 (180) | 408 (208) | This work |
| HCC2700 | 0.83 | 51 (26) | 197 (100) | 409 (208) | 476 (242) | This work |
| HCC2800 | 0.63 | 25 (13) | 116 (59) | 312 (159) | 405 (206) | This work |
| SD2600 | 0.94 | 54 (27) | 178 (91) | 315 (160) | 348 (177) | 1 |
| SD2600P | 0.95 | 80 (41) | 242 (123) | 370 (188) | 399 (203) | 1 |
| SD2650 | 0.89 | 47 (24) | 161 (82) | 294 (150) | 338 (172) | 1 |
| SD2650P | 0.81 | 54 (27) | 189 (96) | 371 (189) | 427 (217) | 1 |
| Carbon A1 | 1.00 | 38 (19) | 157 (80) | 278 (142) | 316 (161) | 2 |
| Carbon A3-36 | 0.87 | 27 (14) | 128 (65) | 302 (154) | 378 (192) | 2 |
| MOF210 | 0.25[b] | 4 (2) | 10 (5) | 38 (19) | 65 (33) | 3 |
| Mg-MOF-74 | 0.41[c] | 103 (52) | 144 (73) | | | 4,5 |

[a] Packing density or tapping density. Packing density of ACC2$T$ and HCC2$T$ carbons may be determined from pellets compacted in a 1.3 cm die for ca. 5 min at 7 MPa. Similar values are obtained from the general equation; $d_{carbon} = (1/\rho_s + V_T)^{-1}$, where $\rho_s$ is skeletal density and $V_T$ is total pore volume from nitrogen sorption analysis. The skeletal density was determined from helium pycnometry. from reference 25. [b] Crystal density of MOF210. [c] 'Tapping density' of Mg-MOF-74 from reference 5.

**References**

1. N. Balahmar, A. C. Mitchell, and R. Mokaya, *Adv. Energy Mater.*, 2015, **5**, 1500867.
2. J. P. Marco-Lozar, M. Kunowsky, F. Suarez-Garcia, J. D. Carruthers and A. Linares-Solano, *Energy Environ. Sci.*, 2012, **5**, 9833.
3. H. Furukawa, N. Ko, Y. B. Go, N. Aratani, S. B. Choi, E. Choi, A. O. Yazaydin, R. Q. Snurr, M. O'Keeffe, J. Kim and O. M. Yaghi, *Science*, 2010, **329**, 424.
4. S. R. Caskey, A. G. Wong-Foy and A. J. Matzger, *J. Am. Chem. Soc.*, 2008, **130**, 10870.
5. Y. Peng, V. Krungleviciute, I. Eryazici, J. T. Hupp, O. K. Farha and T. Yildirim, *J. Am. Chem. Soc.* 2013, **135**, 11887.

Table S3. Volumetric working capacity, expressed as g l$^{-1}$ (or cm$^3$ (STP) cm$^{-3}$) for pressure swing adsorption (PSA) and vacuum swing adsorption (VSA) of $CO_2$ on clove-derived activated carbons compared to benchmark porous materials at ca. 25 $^o$C for a pure $CO_2$ gas stream and a 20% partial $CO_2$ pressure flue gas stream. The values in parentheses are the working capacity in cm$^3$ (STP) cm$^{-3}$

| Sample | Density (g cm$^{-3}$) | Pure $CO_2$[a] (g/l or cm$^3$ cm$^{-3}$) | | Flue gas $CO_2$[b] (g l$^{-1}$ or cm$^3$ cm$^{-3}$) | | Reference |
|---|---|---|---|---|---|---|
| | | PSA | VSA | PSA | VSA | |
| ACC2600 | 0.92 | 231 (118) | 211 (108) | 142 (72) | 73 (37) | This work |
| ACC2700 | 0.79 | 257 (131) | 202 (103) | 139 (71) | 66 (34) | This work |
| ACC2800 | 0.72 | 248 (126) | 162 (82) | 111 (57) | 51 (26) | This work |
| HCC2600 | 0.98 | 185 (94) | 198 (101) | 134 (68) | 86 (44) | This work |
| HCC2700 | 0.83 | 238 (121) | 223 (114) | 153 (78) | 84 (43) | This work |
| HCC2800 | 0.63 | 225 (115) | 144 (73) | 100 (51) | 47 (24) | This work |
| SD2600 | 0.94 | 153 (78) | 190 (97) | 124 (63) | 87 (44) | 1 |
| SD2600P | 0.95 | 142 (72) | 251 (128) | 171 (87) | 121 (62) | 1 |
| SD2650 | 0.89 | 149 (76) | 180 (92) | 121 (62) | 74 (38) | 1 |
| SD2650P | 0.81 | 143 (73) | 213 (108) | 143 (73) | 86 (44) | 1 |
| HKUST-1 | 0.43 | 147 (75) | 121 (62) | 85 (43) | 30 (15) | 2 |
| Mg-MOF-74 | 0.41 | 63 (32) | 70 (36) | 38 (19) | 74 (38) | 2 |
| NaX | 0.63 | 44 (22) | 78 (40) | 50 (26) | 69 (35) | 3 |

[a]1 bar to 6 bar for PSA; 0.05 bar to 1.5 bar for VSA. [b]0.2 bar to 1.2 bar for PSA; 0.01 bar to 0.3 bar for VSA.

**References**
1. N. Balahmar, A. C. Mitchell, and R. Mokaya, *Adv. Energy Mater.*, 2015, **5**, 1500867.
2. J. M. Simmons, H. Wu, W. Zhou and T. Yildirim, *Energy Environ. Sci.*, 2011, **4**, 2177.
3. Y. Belmabkhout, G. Pirngruber, E. Jolimaitre and A. Methivier, *Adsorption*, 2007, **13**, 341.

Table S4. Methane uptake for compacted activated carbons compared to selected benchmark MOFs and carbons reported in the literature. Volumetric uptake of powder MOFs is calculated

| Sample | Density (g cm$^{-3}$) | 65 bar (g g$^{-1}$) | 65 bar (cm$^3$ cm$^{-3}$) | 80 bar (g g$^{-1}$) | 80 bar (cm$^3$ cm$^{-3}$) | 100 bar (g g$^{-1}$) | 100 bar (cm$^3$ cm$^{-3}$) | Reference |
|---|---|---|---|---|---|---|---|---|
| CHCC2800 | 0.82 | 0.26 | 293 | 0.28 | 315 | 0.30 | 339 | This work |
| CHCC4700 | 0.75 | 0.27 | 282 | 0.29 | 306 | 0.32 | 334 | This work |
| CHCC4800 | 0.58 | 0.32 | 258 | 0.35 | 279 | 0.38 | 309 | This work |
| CNL4800 | 0.67 | 0.26 | 241 | 0.29 | 269 | 0.31 | 291 | 1 |
| PPYCNL124 | 0.52 | 0.30 | 217 | 0.33 | 238 | 0.36 | 260 | 1 |
| PPYCNL214 | 0.36 | 0.36 | 183 | 0.41 | 204 | 0.46 | 229 | 1 |
| ACDS4800 | 0.69 | 0.25 | 243 | 0.27 | 262 | 0.29 | 282 | 1,2 |
| PPYSD114 | 0.47 | 0.32 | 211 | 0.35 | 231 | 0.39 | 254 | 1 |
| AX-21 carbon | 0.487 | 0.30 | 203 | 0.33 | 222 | 0.35 | 238 | 3 |
| HKUST-1 | 0.881 | 0.21 | 263 | 0.22 | 272 | 0.23 | 281 | 3 |
| Ni-MOF-74 | 1.195 | 0.15 | 259 | 0.16 | 267 | 0.17 | 277 | 3 |
| Al-soc-MOF-1 | 0.34 | 0.41 | 197 | 0.47 | 222 | | | 4 |
| MOF-210 | 0.25 | 0.41 | 143 | 0.48 | 168 | | | 5 |
| NU-1500-Al | 0.498 | 0.29 | 200 | 0.31 | 216 | 0.34 | 237 | 6 |
| NU-1501-Fe | 0.299 | 0.40 | 168 | 0.46 | 193 | 0.52 | 218 | 6 |
| NU-1501-Al | 0.283 | 0.41 | 163 | 0.48 | 190 | 0.54 | 214 | 6 |
| monoHKUST-1 | 1.06 | 0.17 | 261 | 0.18 | 278 | 0.18 | 275 | 7 |
| monoUiO-66_D | 1.05 | 0.14 | 210 | 0.17 | 245 | 0.20 | 296 | 8 |

based on crystallographic density rather than packing density.

**References**
1. A. Altwala and R. Mokaya, *J. Mater. Chem. A*, 2022, **10,** 13744.
2. A. Altwala and R. Mokaya, *Energy Environ. Sci.*, 2020, **13**, 2967.
3. J. A. Mason, M. Veenstra and J. R. Long, *Chem. Sci.*, 2014, **5**, 32.
4. D. Alezi, Y. Belmabkhout, M. Suyetin, P. M. Bhatt, Ł. J. Weseliński, V. Solovyeva, K. Adil, I. Spanopoulos, P. N. Trikalitis, A.-H. Emwas, M. Eddaoudi, *J. Am. Chem. Soc.,* 2015, **137**, 13308.
5. H. Furukawa, N. Ko, Y. B. Go, N. Aratani, S. B. Choi, E. Choi, A. O. Yazaydin, R. Q. Snurr, M. O'Keeffe, J. Kim, O. M. Yaghi, *Science* 2010, **329**, 424–428.
6. Z. Chen, P. Li, R. Anderson, X. Wang, X. Zhang, L. Robison, L. R. Redfern, S. Moribe, T. Islamoglu, D. A. Gómez-Gualdrón, T. Yildirim, J. F. Stoddart and O. K. Farha, *Science*, 2020, **368**, 297.
7. T. Tian, Z. Zeng, D. Vulpe, M. E. Casco, G. Divitini, P. A. Midgley, J. Silvestre-Albero, J. C. Tan, P. Z. Moghadam and D. Fairen-Jimenez, *Nat. Mater.*, 2018, **17**, 174.
8. B. M. Connolly, M. Aragones-Anglada, J. Gandara-Loe, N. A. Danaf, D. C. Lamb, J. P. Mehta, D. Vulpe, S. Wuttke, J. Silvestre-Albero, P. Z. Moghadam, A. E. H. Wheatley and

D. Fairen-Jimenez, *Nat. Commun.*, 2019, **10**, 2345.

Table S5: Methane uptake working capacity for compacted activated carbons compared to selected benchmark MOFs and carbons reported in the literature.

| Sample | 65 bar | | 80 bar | | 100 bar | | Reference |
| | $(g\ g^{-1})$ | $(cm^3\ cm^{-3})$ | $(g\ g^{-1})$ | $(cm^3\ cm^{-3})$ | $(g\ g^{-1})$ | $(cm^3\ cm^{-3})$ | |
|---|---|---|---|---|---|---|---|
| CHCC2800 | 0.18 | 200 | 0.20 | 222 | 0.22 | 246 | This work |
| CHCC4700 | 0.20 | 210 | 0.22 | 234 | 0.25 | 262 | This work |
| CHCC4800 | 0.25 | 197 | 0.28 | 218 | 0.31 | 248 | This work |
| CNL4800 | 0.19 | 182 | 0.22 | 202 | 0.24 | 224 | 1 |
| PPYCNL124 | 0.23 | 167 | 0.26 | 188 | 0.29 | 209 | 1 |
| PPYCNL214 | 0.29 | 146 | 0.34 | 167 | 0.39 | 192 | 1 |
| ACDS4800 | 0.18 | 171 | 0.20 | 189 | 0.22 | 209 | 1,2 |
| PPYSD114 | 0.25 | 162 | 0.28 | 182 | 0.32 | 205 | 1 |
| AX-21 carbon | 0.23 | 155 | 0.26 | 174 | 0.28 | 190 | 3 |
| HKUST-1 | 0.15 | 179 | 0.16 | 198 | 0.17 | 207 | 3 |
| Ni-MOF-74 | 0.08 | 148 | 0.09 | 152 | 0.10 | 162 | 3 |
| Al-soc-MOF-1 | 0.36 | 176 | 0.42 | 201 | | | 4 |
| MOF-210 | 0.38 | 134 | 0.45 | 157 | | | 5 |
| NU-1500-Al | 0.24 | 165 | 0.26 | 181 | 0.29 | 202 | 6 |
| NU-1501-Fe | 0.36 | 151 | 0.42 | 176 | 0.48 | 201 | 6 |
| NU-1501-Al | 0.37 | 147 | 0.44 | 174 | 0.50 | 198 | 6 |
| monoHKUST-1 | 0.12 | 184 | 0.13 | 201 | 0.13 | 198 | 7 |
| monoUiO-66_D | 0.11 | 167 | 0.14 | 202 | 0.17 | 253 | 8 |

**References**
1. A. Altwala and R. Mokaya, *J. Mater. Chem. A*, 2022, **10,** 13744.
2. A. Altwala and R. Mokaya, *Energy Environ. Sci.*, 2020, **13**, 2967.
3. J. A. Mason, M. Veenstra and J. R. Long, *Chem. Sci.*, 2014, **5**, 32.
4. D. Alezi, Y. Belmabkhout, M. Suyetin, P. M. Bhatt, Ł. J. Weseliński, V. Solovyeva, K. Adil, I. Spanopoulos, P. N. Trikalitis, A.-H. Emwas, M. Eddaoudi, *J. Am. Chem. Soc.,* 2015, **137**, 13308.
5. H. Furukawa, N. Ko, Y. B. Go, N. Aratani, S. B. Choi, E. Choi, A. O. Yazaydin, R. Q. Snurr, M. O'Keeffe, J. Kim, O. M. Yaghi, *Science* 2010, **329**, 424–428.
6. Z. Chen, P. Li, R. Anderson, X. Wang, X. Zhang, L. Robison, L. R. Redfern, S. Moribe, T. Islamoglu, D. A. Gómez-Gualdrón, T. Yildirim, J. F. Stoddart and O. K. Farha, *Science*, 2020, **368**, 297.
7. T. Tian, Z. Zeng, D. Vulpe, M. E. Casco, G. Divitini, P. A. Midgley, J. Silvestre-Albero, J. C. Tan, P. Z. Moghadam and D. Fairen-Jimenez, *Nat. Mater.*, 2018, **17**, 174.
8. B. M. Connolly, M. Aragones-Anglada, J. Gandara-Loe, N. A. Danaf, D. C. Lamb, J. P. Mehta, D. Vulpe, S. Wuttke, J. Silvestre-Albero, P. Z. Moghadam, A. E. H. Wheatley and

D. Fairen-Jimenez, *Nat. Commun.*, 2019, **10**, 2345.

Scheme S1: Schematic showing the steps in the carbonisation of raw cloves via the flash air carbonisation route to yield air carbonised clove (ACC) carbon, which was used as starting material for activation to yield ACC*xT* series of activated carbons (where *x* in KOH/ACC ratio and *T* is activation temperature.

**Flash Air carbonisation**

400 °C/5-10 minutes in air

**Raw Cloves**

**Air carbonised clove (ACC)**

Sample in alumina boat

$N_2$ or Air

Oven controls

Ramp rate °C/min
Target Temperature °C
Holding time- hour
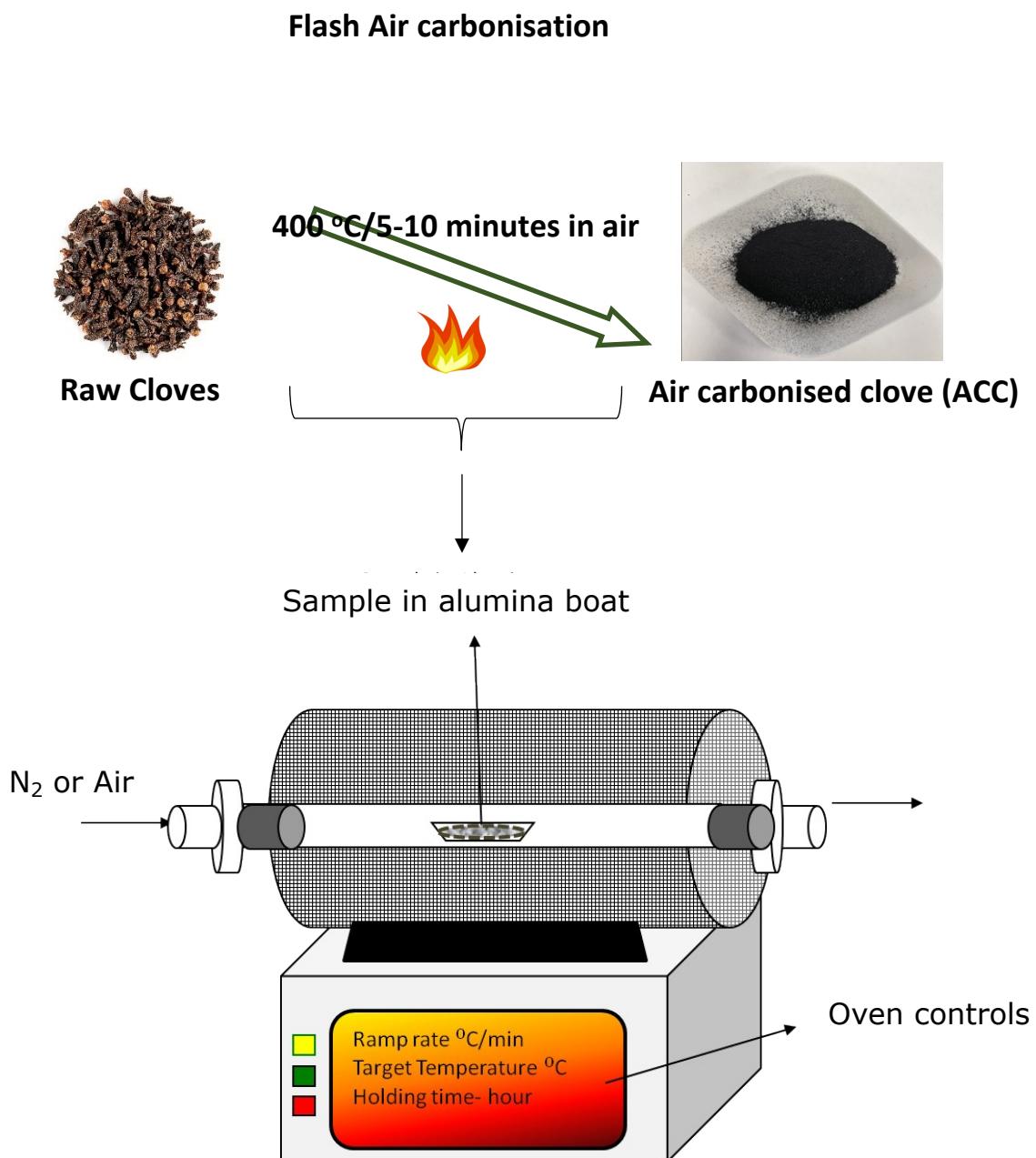
Scheme S2: Schematic showing the steps in the carbonisation of raw cloves via the hydrothermal carbonisation route to yield clove hydrochar (HCC), which was used as starting material for activation to yield HCC*x*T series of activated carbons (where *x* in KOH/HCC ratio and *T* is activation temperature.

**Hydrothermal carbonisation**

**250 °C/2 hours in water**

**Raw Cloves**

**Clove hydrochar (HCC)**

**Hydrothermal bomb reactor**
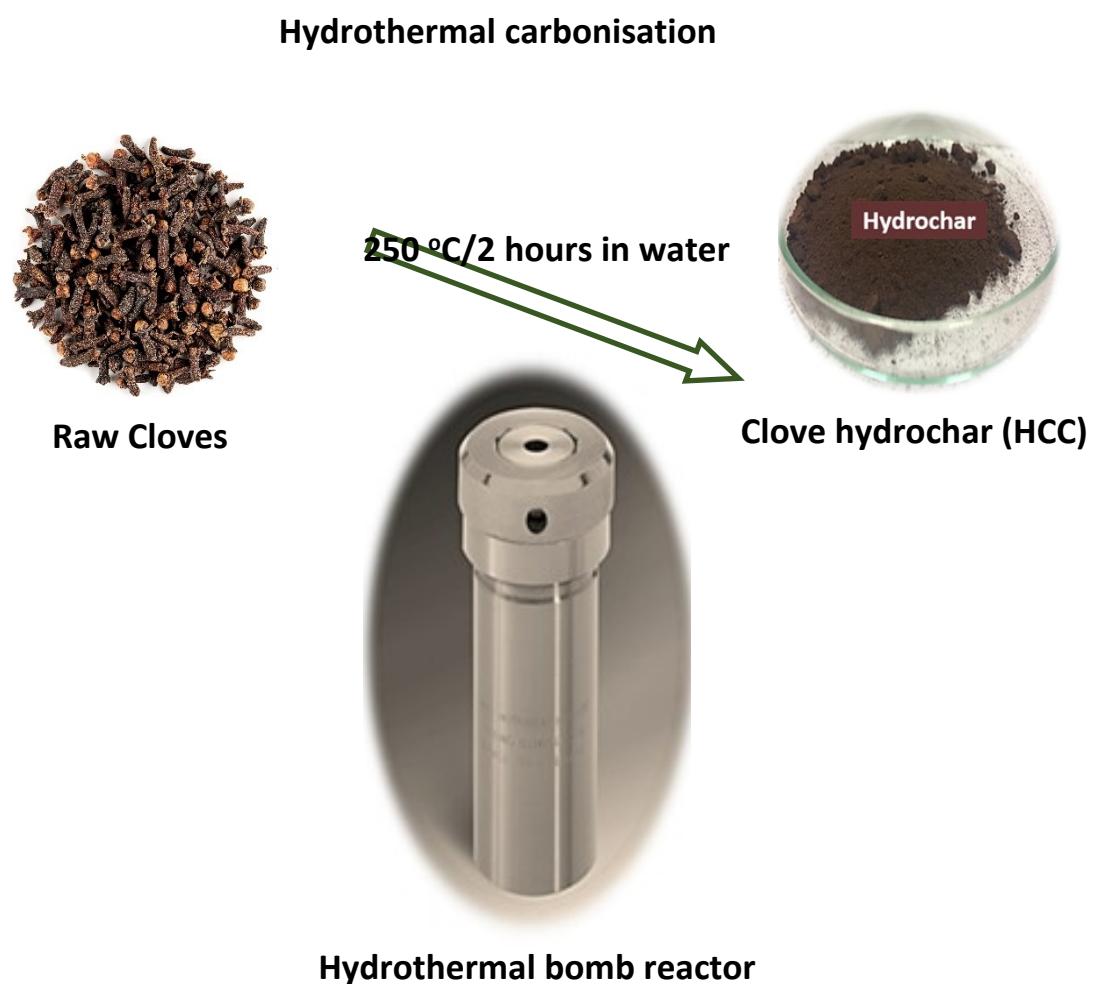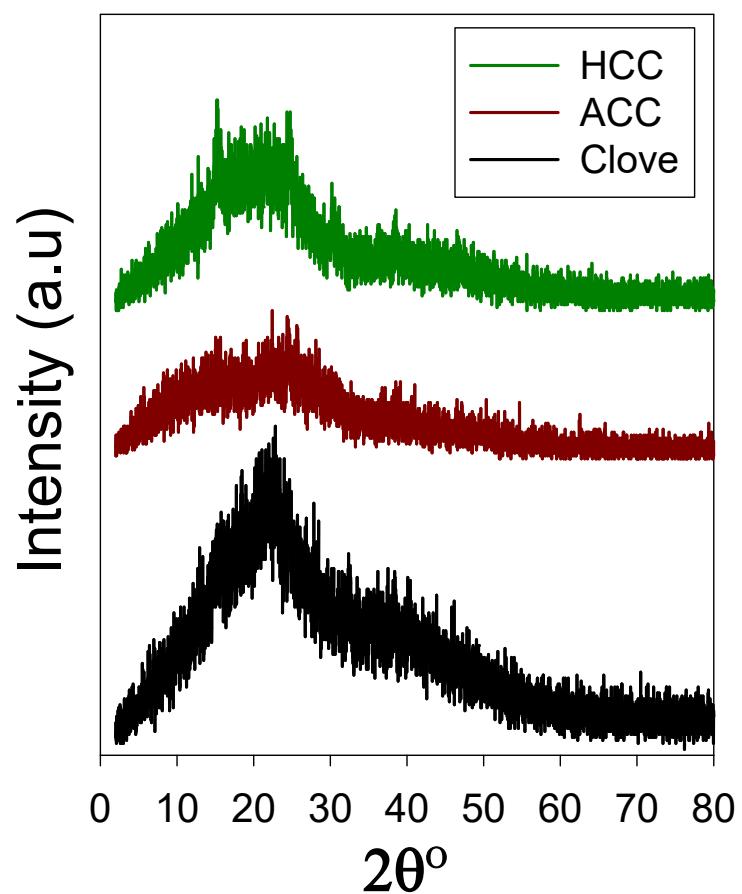
Figure S1. Powder XRD patterns of raw clove, air-carbonised clove (ACC) and clove hydrochar (HCC).
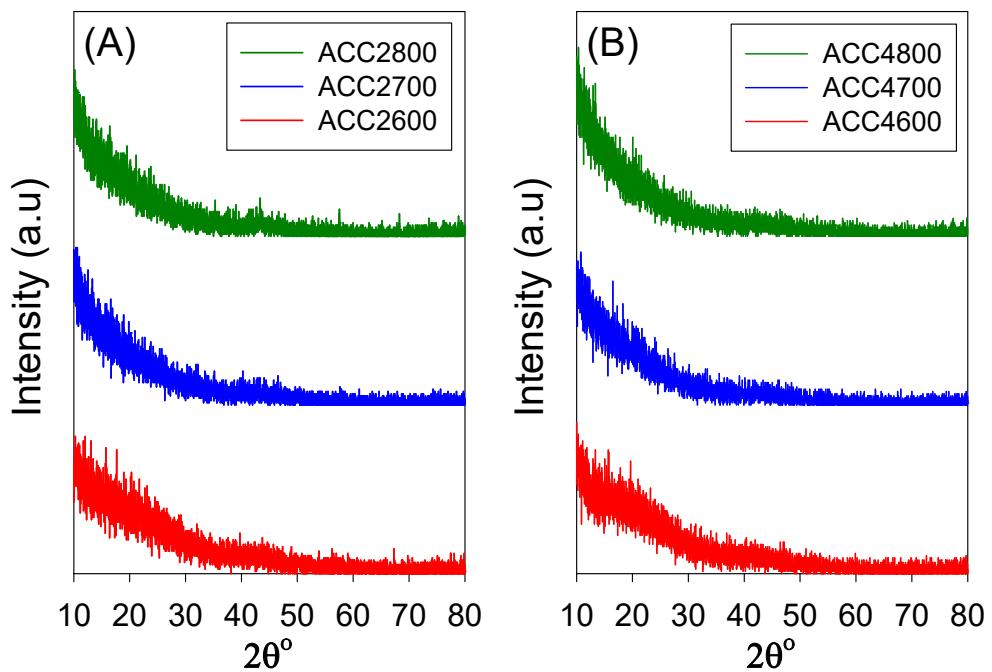
Figure S2. Powder XRD patterns of activated carbons derived from air-carbonised clove (ACC).
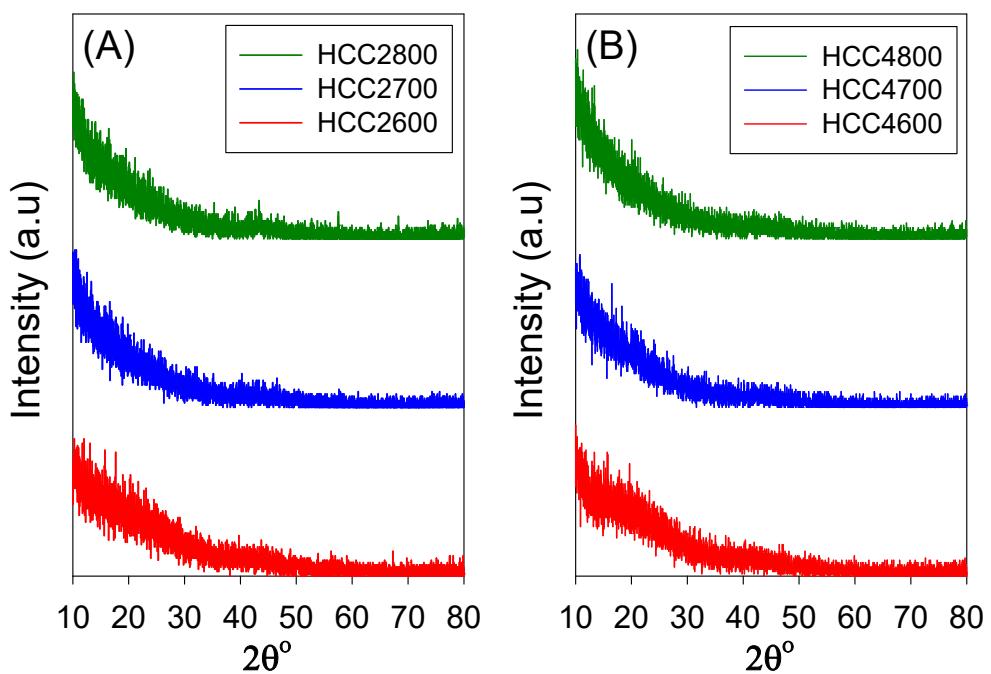
Figure S3. Powder XRD patterns of activated carbons derived from clove hydrochar (HCC).
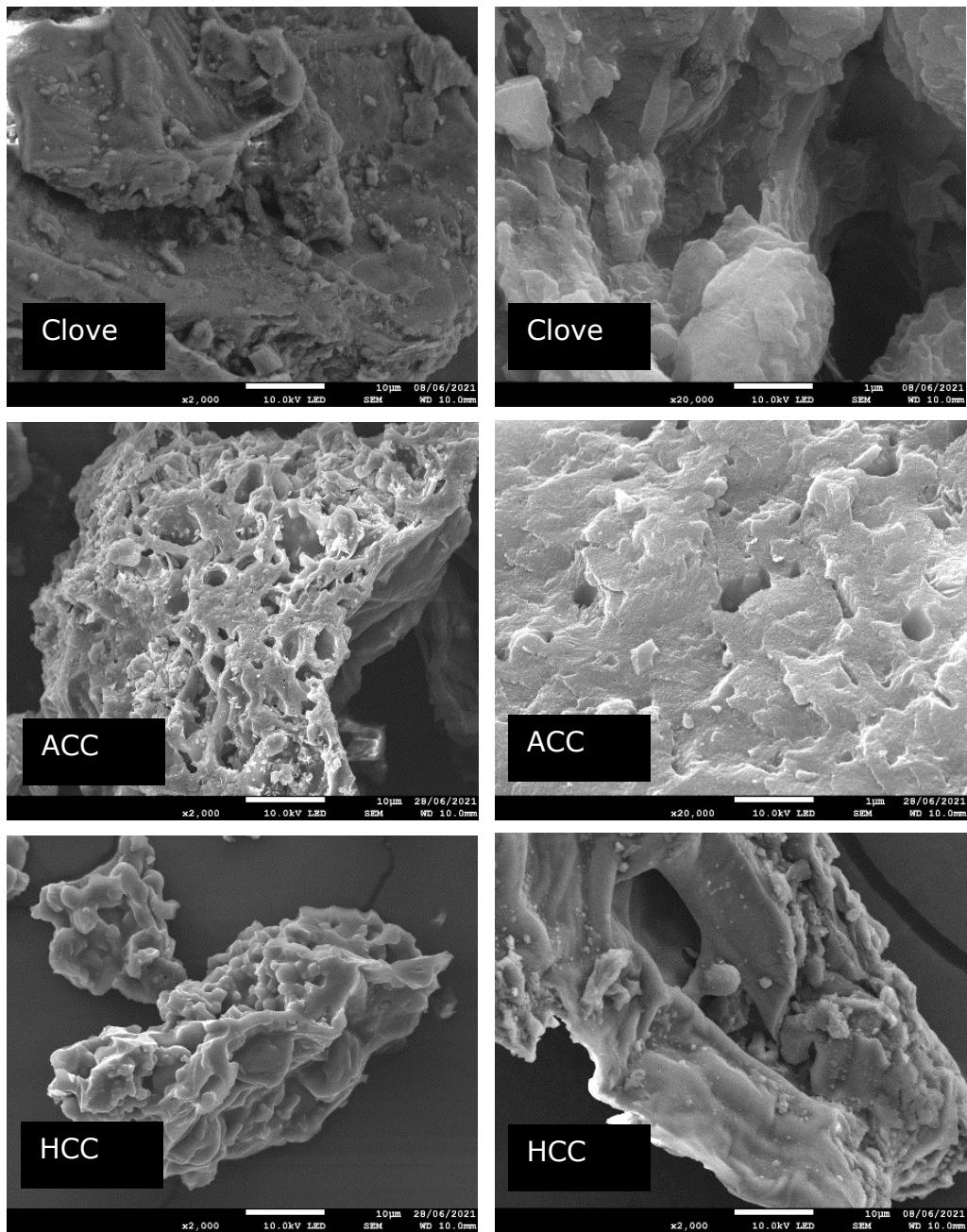
Figure S4. SEM images of raw clove, air-carbonised clove (ACC) and clove-derived hydrochar (HCC).
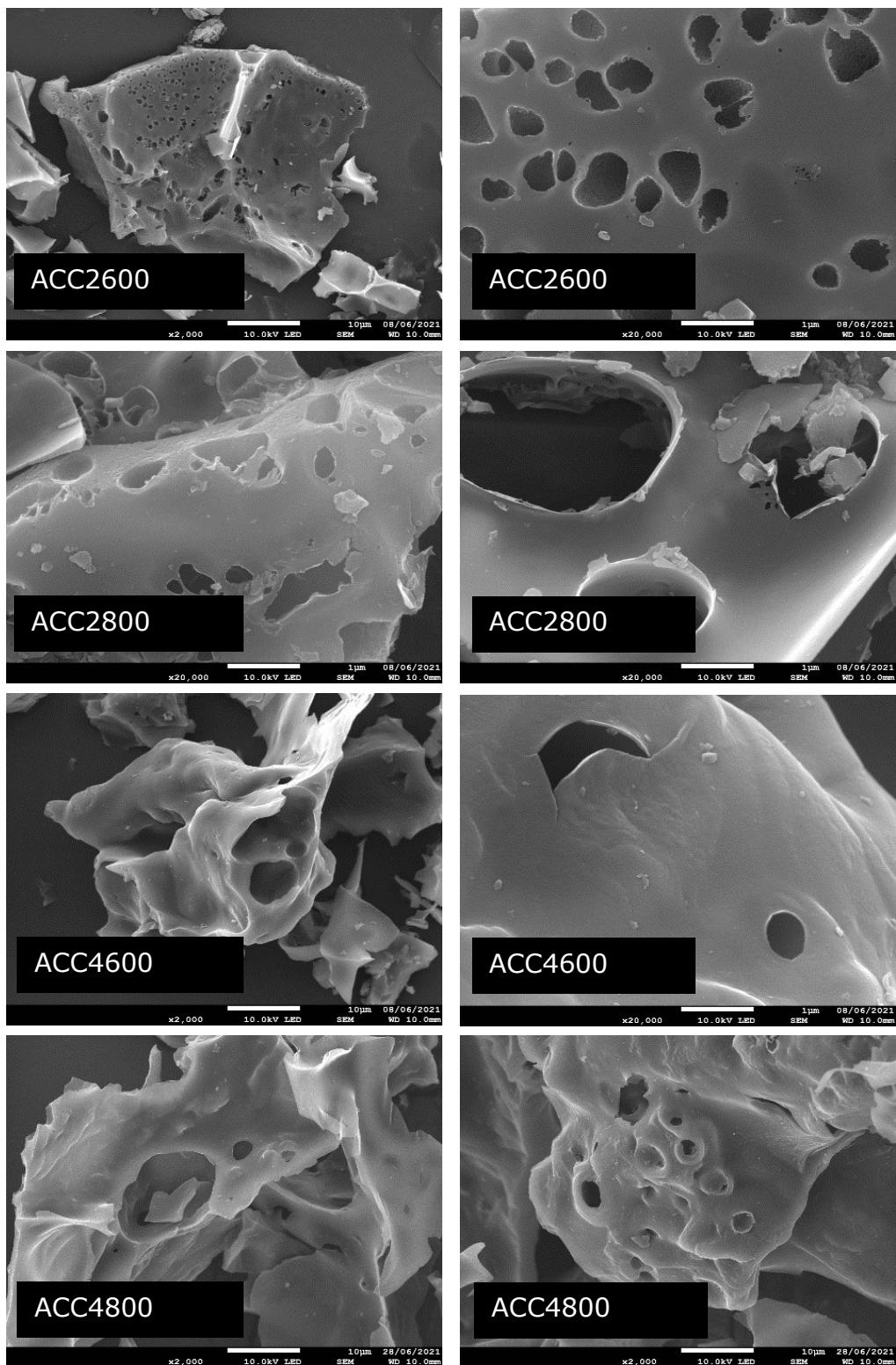
Figure S5. Representative SEM images of activated carbons derived from air-carbonised clove.
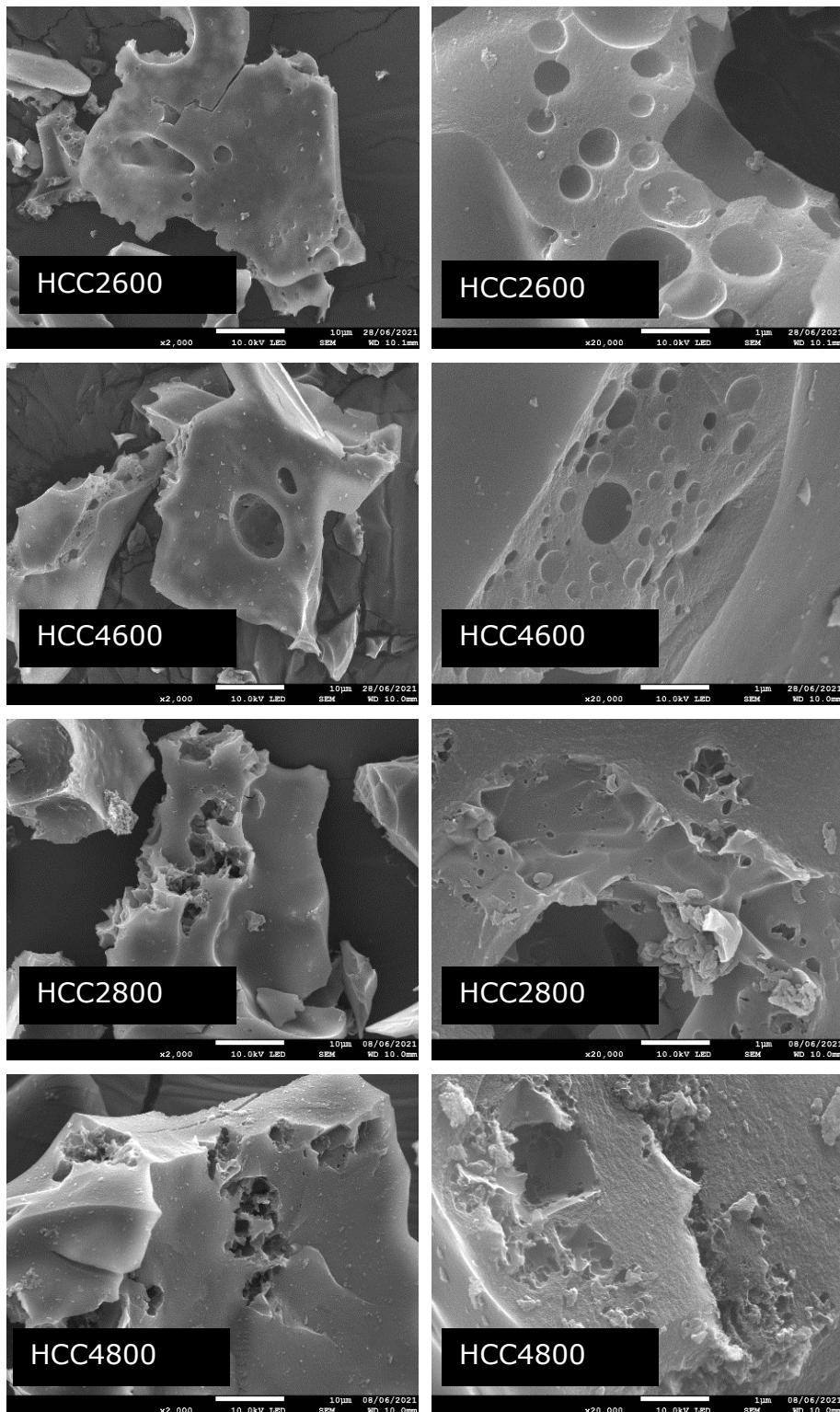
Figure S6. Representative SEM images of activated carbons derived from clove hydrochar.
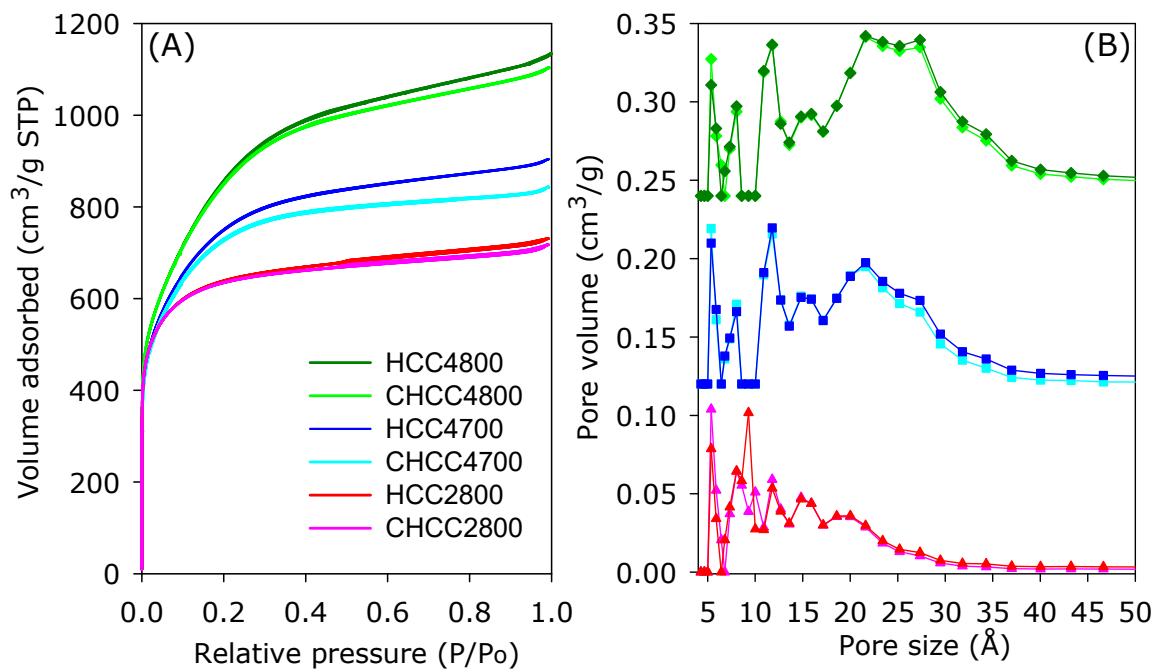
Figure S7. A comparison of representative hydrochar-derived carbons before and after compaction; (A) Nitrogen sorption isotherms and (B) pore size distribution (PSD) curves.
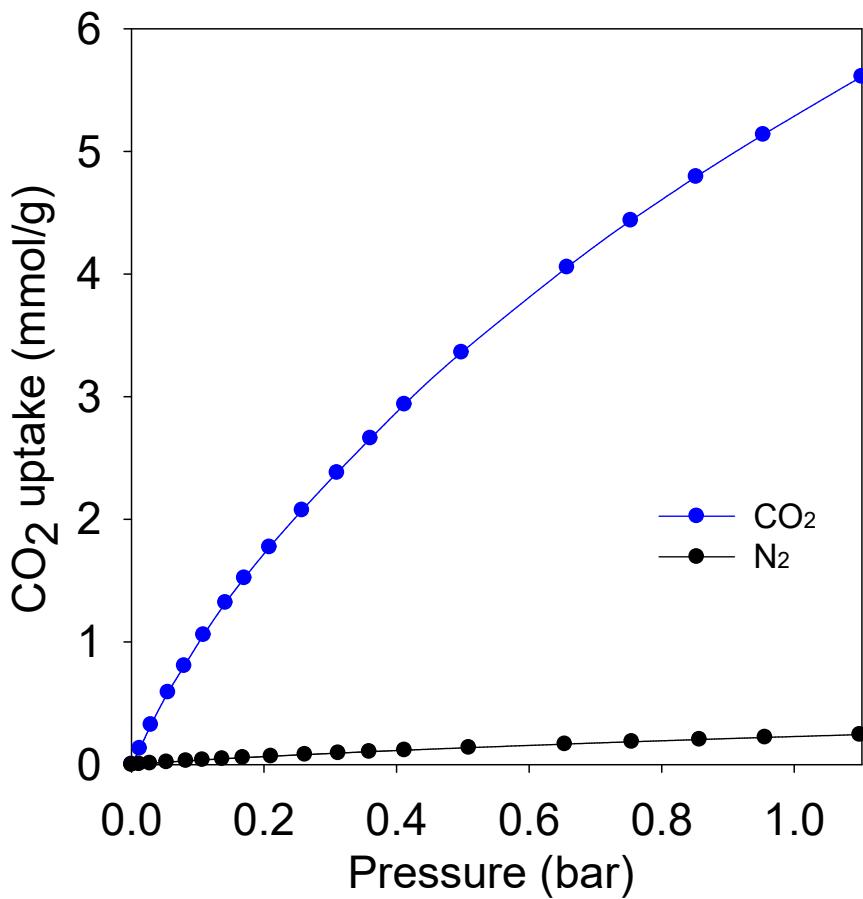
Figure S8. Comparison of $CO_2$ and $N_2$ uptake at room temperature for sample HCC2700. The $CO_2/N_2$ adsorption ratio is 22 at 1 bar.
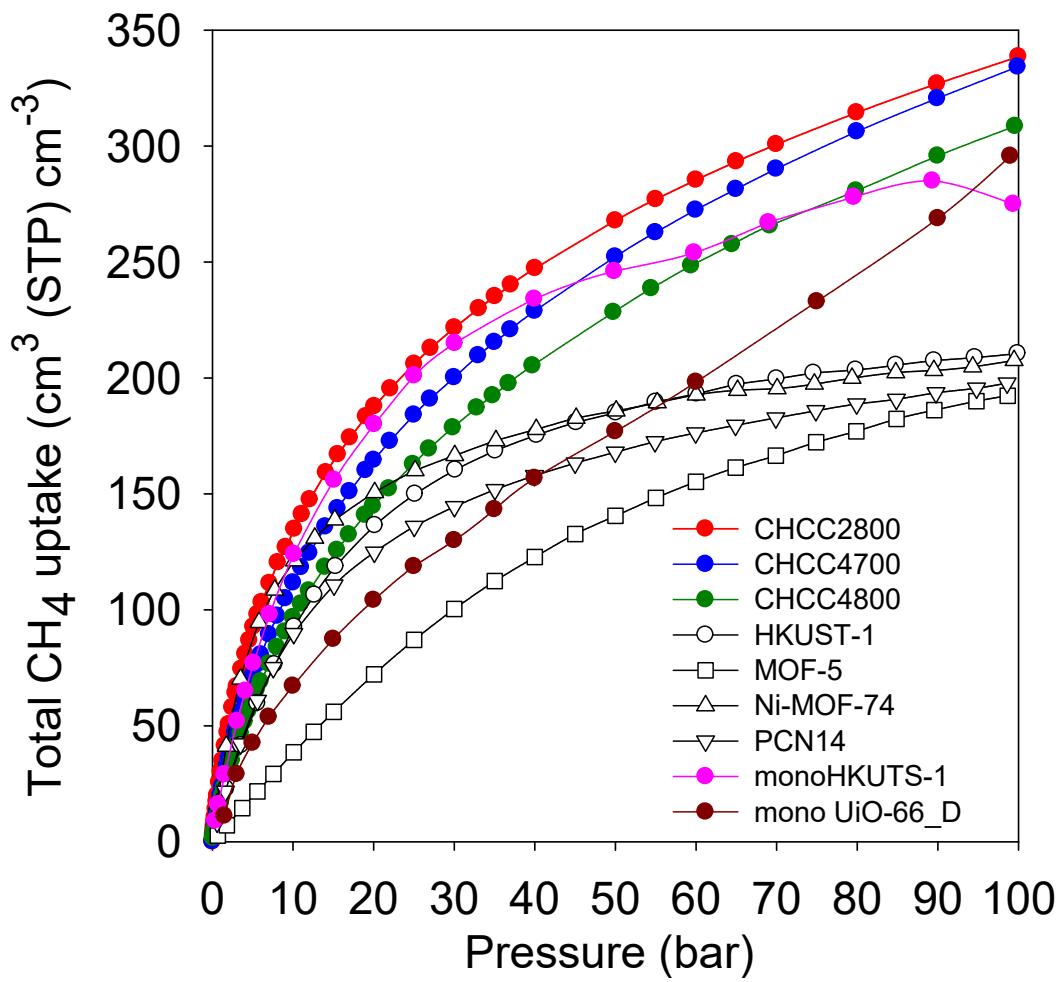
Figure S9. Total volumetric methane uptake of compacted activated carbons at 25 °C compared to benchmark MOF materials. The uptake of powder MOFs was calculated using crystallographic density and a reduction of 25% was applied to simulate more realistic packing density.